

PAPER • OPEN ACCESS

The effect of rectangular gurney flap on wells turbine performance

To cite this article: A T Kotb *et al* 2020 *IOP Conf. Ser.: Mater. Sci. Eng.* **973** 012006

View the [article online](#) for updates and enhancements.

You may also like

- [Performance Simulation of Tubular Segmented-in-Series SOFC Using Simplified Equivalent Circuit](#)
Shun Yoshida, Tadashi Tanaka and Yoshitaka Inui
- [\(Invited\) Potential of Double Network Gel as a Tribological Material Realizing Low Friction in Water](#)
Koki Kanda and Koshi Adachi
- [Analysis of the Effect of Surface Diffusion on Effective Diffusivity of Oxygen in Catalyst Layer By Direct Simulation Monte Carlo](#)
Tomoki Hori, Takuya Mabuchi, Ikuya Kinefuchi et al.



The banner features a dark blue background on the left with white and orange text, and a photograph of a woman at a podium on the right. The woman is smiling and looking towards the camera. The background of the photo is a bright, modern interior with large windows.

 The Electrochemical Society
Advancing solid state & electrochemical science & technology

243rd Meeting with SOFC-XVIII

Boston, MA • May 28 – June 2, 2023

Accelerate scientific discovery!

[Learn More & Register](#)

The effect of rectangular gurney flap on wells turbine performance

A T Kotb¹, M A Nawar² and R M Abd El Maksoud³

¹Demonstrator, Mechanical Power Engineering Department, Faculty of Engineering, Mattaria, Helwan University, Egypt.

²Assist.Prof., Mechanical Power Engineering Department, Faculty of Engineering, Mattaria, Helwan University, Egypt.

³ Assoc. Prof., Mechanical Power Engineering Department, Faculty of Engineering, Mattaria, Helwan University, Egypt.

ahmedtarekmostafa15@gmail.com

Abstract. Wells turbine is very adept at converting pneumatic power from ocean waves into mechanical energy. However, such turbines incur from low performance, limited operating range and low efficiency. The present study introduces a method to enhance the power produced from Wells turbine by implementing rectangular Gurney flap (GF). The Gurney flap is placed on both pressure and suction sides of the trailing edge (TE) and perpendicular to the chord line without change chord length. GF increases the lift coefficient by altering the Kutta condition at the TE. The turbine performance is herein evaluated by solving numerically 3D incompressible Reynolds Averaged Navier–Stokes equations (RANS) by using ANSYS Fluent 19.0. The performance is demonstrated according to the flow coefficient, torque coefficient, total pressure loss coefficient, and the turbine efficiency, as well as the velocity and pressure fields around the turbine blades. The validation of the present work was achieved using previous experimental work and CFD work by using SST $k - \omega$ turbulence model. The present work showed that the Wells turbine augmented with GF increases the torque coefficient by 41.98%. Besides, the stall has been delayed compared with the conventional Wells turbine.

1. Introduction

Wells turbine is utilized to convert ocean wave energy into a mechanical power. It is environmentally device friendly so researchers around the world are investigating on how to boost its performance. Different designs were experimentally studied by Gato et al. [1] and Curran and Gato [2] to investigate the effect of their designs on performance of turbine. Kim et al. [3] made a numerical simulation to study the blade sweep and its effect on the turbine performance. Setoguchi et al. [4,5] introduced influence of self-rectifying turbines and utilizing of inlet guide vanes on design parameters of turbine. Brito-Melo et al. [6] studied numerically different turbine design parameters. Dhanasekaran and Govardhan [7] introduced a numerical study for turbine performance. The effect of inlet conditions on the Wells turbine performance was introduced by Raghunathan et al. [8]. The previous studies confirmed that geometrical parameters such as blade geometry [9], blade setting angle [10], the use of end plates [11] and tip clearance [12] affect Wells turbine performance.

The previous studies showed that the optimum blade profile was found to be NACA0020 for small-scale Wells turbine [13], while the optimum blade profile was NACA0015 for large-scale turbines [14]. The effect of guide vanes on the constant chord Wells turbine was showed by Thakker et al. [15]. Besides, Setoguchi and Takao [16] introduced its effect on the variable chord. A study by [14,17] had



Content from this work may be used under the terms of the [Creative Commons Attribution 3.0 licence](https://creativecommons.org/licenses/by/3.0/). Any further distribution of this work must maintain attribution to the author(s) and the title of the work, journal citation and DOI.

been demonstrated that Wells turbine with guide vanes stalled before those without guide vanes. The effect of tip leakage flow on the Wells turbine performance was showed by Taha et al. [18,19] with uniform tip clearance [18] and also with non-uniform tip clearance [19]. Both studies showed that tip leakage flow effect on the performance of wells turbine and turbine stalling. The influence of geometry of turbine duct on its performance was numerically studied by Shaaban and Hafiz [20]. Halder and Samad [21] showed that the casing treatment influence the vortex pattern which result in stall limit change.

The effect of a number of rotor blades on the wells turbine performance had been studied through many researchers. Some of the previous studies recommended the use of eight rotor blades [1,2,12,22] and others recommended the use of six rotor blades [22,13]. On the other side, using air turbines to be immersed in water gave a promising performance. Hamed et al. [23] proved that operating wells turbine as a hydraulic turbine achieves better performance. The circumferential casing groove (rectangular shape) effects on the turbine performance at different groove depth and width were demonstrated by Halder et al [24]. Moreover, two different cases, with and without a tip groove, were considered to guess the optimal turbine speed for the different flow velocities [25].

The design with grooved-casing performs better than that of the without grooved casing. Using variable blade sweep angles at the tip and mid sections enhanced Wells turbine performance and provided higher range of operating [26, 27]. Torres FR, et al [28] demonstrated a methodology to determine the optimal size of a Wells turbine taking into account hydro-aerodynamic model. Moreover, Nazeryan M, et al [29] investigated numerically the influence of blade thickness on both aerodynamic and entropy generation analysis of a Wells turbine. Besides, Gratton T, et al [30] performed for optimizing the blade profile in the Wells turbine for better performance, by the torque coefficient magnification. Kumar and Samad [31] showed the effect of rectangular flap and flap height on wells turbine performance.

In accordance to previous researches, still much effort is needed to boost Wells turbine performance that incurs from low performance, limited operating range and low efficiency. Accordingly, the goal of the present paper is to overcome these disadvantages. The present study introduces a method to enhance the power produced from Wells turbine by implementing different geometries of Gurney flap (GF). The Gurney flap is placed on both pressure and suction sides of the trailing edge (TE) and perpendicular to the chord line without change chord length.

Wells turbine is investigated while having symmetrical NACA 0015 blades. The turbine performance is here in evaluated by solving numerically 3D incompressible Reynolds Averaged Navier–Stokes equations (RANS) by using ANSYS Fluent 19.0. The performance is demonstrated according to the flow coefficient, torque coefficient, total pressure loss coefficient, and the turbine efficiency, as well as the velocity and pressure fields around the turbine blades. The choice of the number of blades used is rationalized from previous studies.

2. Computational methodology

In this section, Wells turbine theory of operation, its gurney flap and its computational methodology are showed.

2.1. Wells turbine

Wells turbine is one of the most important Ocean-wave energy converters that convert Ocean-wave energy into mechanical power. Actually, in oscillation water column (OWC) wave energy converters, pressure fluctuations are generated due to motion of wave, inside a plenum, and therefore producing an oscillating air-flow, so the self-rectifying Wells turbine can efficiently convert whose energy into a unidirectional rotational motion; see figure.1a. In its basic arrangement, this is an axial-flow air turbine, consisting of a rotor with a number of symmetrical and untwisted airfoil blades, usually coding to the NACA00XX series, usually chord line is perpendicular to rotational axis (90 ° stagger angle); see figure 1b, [12].

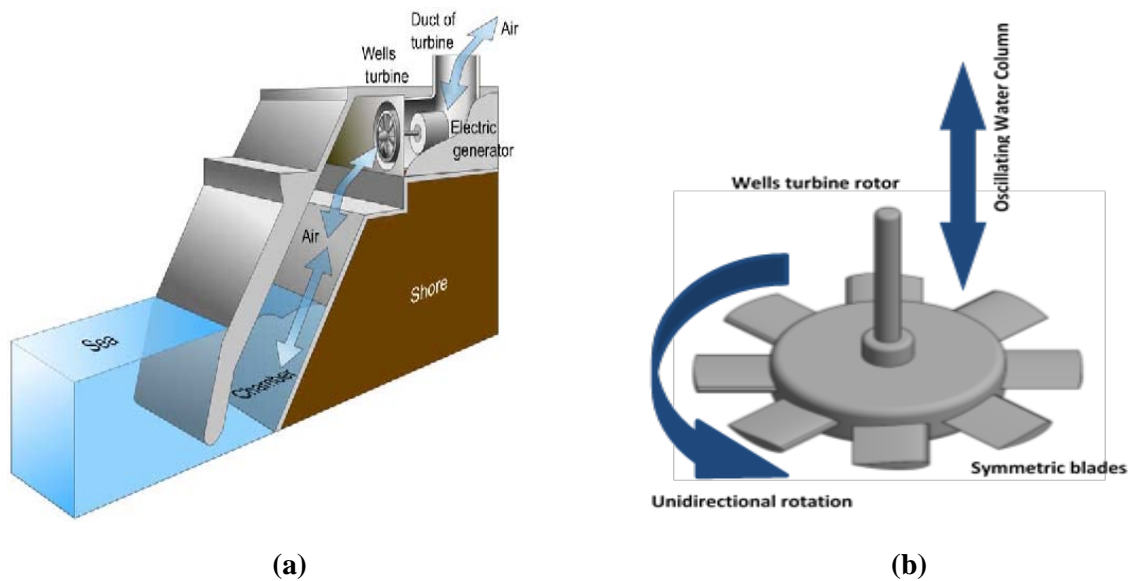


Figure1. (a) Schematic cutaway of a Wells turbine, (b) The Wells air turbine.

2.2. Gurney flap scheme

The present study introduces a method to enhance the power produced from Wells turbine by implementing different geometries of Gurney flap (GF). The Gurney flap is placed on both pressure and suction sides of the trailing edge (TE) and perpendicular to the chord line without change chord length. In the present study, a rectangular Gurney flap (GF) is studied, see figure 2. In this paper a rectangular Gurney flap (GF) height was varied from 0.5-2% C and the width from 0.4-0.6% C.

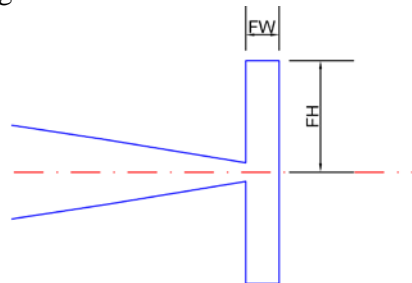


Figure2. Schematic of rectangular Gurney flap.

2.3. Computational equations

In figure 3, the flow having an angle of incidence (α) will produce a lift force (L) and a drag force (D). The components of these forces in both tangential and axial directions are denoted by F_t and F_a , respectively. Accordingly, F_t generates torque on the turbine rotor, while F_a produces axial stress on the rotor as a result of thrust force on the turbine rotor axis [7]. Accordingly, for wells turbine in an oscillating airflow, the angle of incidence (α) changes from positive to negative values in accordance with the upward and downward directions of flow, respectively; see figure 1. The tangential force F_t is acting in the same direction regardless of the positive or negative value of an angle of incidence (α) because of symmetry of the rotor blade.

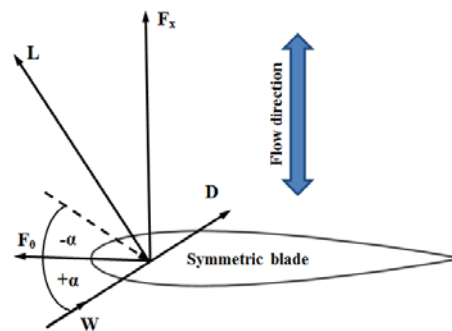


Figure 3. Forces acting on a Wells turbine blade.

In accordance with, torque has a unidirectional feature that is created from an oscillating flow [7]. The flow coefficient, ϕ , can be introduced as:

$$\phi = \frac{C_x}{U} \quad (1)$$

The flow coefficient is changed in accordance with the variation of the axial flow velocity C_x while keeping the rotor tip speed U constant. Thus, the torque coefficient C_T can be introduced as:

$$C_T = \frac{T}{\rho \omega^2 R_T^5} \quad (2)$$

where T the torque on rotor is, ρ is the working fluid density, ω is the angular velocity of turbine and R_T is the radius of rotor tip. Total pressure drop coefficient C_P is expressed by the following formula:

$$C_P = \frac{\Delta P_0}{\rho \omega^2 R_T^2} \quad (3)$$

Where ΔP_0 is the total pressure drop.

The Turbine efficiency (η) is introduced as:

$$\eta = \frac{T\omega}{\Delta P_0 Q} \quad (4)$$

where Q is the volume flow rate through the turbine.

Rotor solidity is an important parameter that affects the performance of Wells turbines. The rotor solidity σ is defined as:

$$\sigma = \frac{Z * c * H}{\pi * (R_T^2 - R_h^2)} = \frac{Zc}{2\pi R_m} \quad (5)$$

where Z is the number of blades, c is the chord length; H is the blade height, R_T is the radius of rotor tip, R_h is the radius of rotor hub and R_m is the turbine mean radius. Eq. (5), shows that the rotor solidity σ can be varied by change the number of turbine blades.

In the present study, the influence of using different geometries of Gurney flap (GF) on performance of Wells turbine is numerically investigated by solving the 3D incompressible Reynolds-averaged Navier-Stokes equations RANS for wells turbine with Gurney flap (GF). The basic purpose of using any turbulence model is to bring results closer to the experimental results. In this study, the SST $k-\omega$ Turbulence model is used. In addition, Non-dimensional wall distance $y^+ < 1$ to guess flow pattern on buffer and sub-layer zones. The good prediction of the aerodynamic performance was achieved by the combination of the SST $k-\omega$ Turbulence model with non-dimensional wall distance $y^+ < 1$. Besides, the Moving Reference Frame method (MRF) is applied to simulate the

turbine rotor, but the main governing equations are solved in the absolute frame. The finite volume method is applied to appreciate the absolute frame using the computational fluid dynamics (CFD) code ‘‘Fluent’’ V19.0. The present simulation uses different discretization methods. These methods are shown in the following table; see table 1:

Table 1. Solution methods.

Pressure-velocity coupling	SIMPLEC
Gradient	Least squares cell based
Pressure	Standard
Momentum	The second order upwind
Turbulent kinetic energy(k)	The second order upwind
Specific dissipation rate(ω)	The second order upwind

The SIMPLEC algorithm applied for pressure-velocity coupling eliminates the influence of mesh skewness on the final solution. The maximum residual values for momentum, continuity, velocity x, velocity y, velocity z and turbulence equations of the solutions are 10^{-4} . Moreover, the value of turbulence intensity at inlet and outlet is 5% (The turbulence intensity is defined as the ratio of the root-mean-square of the velocity fluctuations to the mean flow velocity).

3. Results and discussions

In this part four parts are presented and they are a mesh size independence study, model validation, effect of different geometries of Gurney flap on turbine performance, and the field of flow around the blades.

3.1. Mesh independent study

Curran and Gato [2] wells turbine dimensions are used in this investigation. The specifications of the Wells turbine that is under study are shown in table 1. The full cylindrical domain of eight-blade rotor is reduced to slice of domain angle $\theta = \frac{360}{8} = 45^\circ$ of the full domain, see figure 4. This minimized was made on account of the rotor of turbine symmetry around the axis of rotational and as a result, the computational time is reduced [20]. Besides, table 2 presents domain meshing and domain boundary conditions. Figure 4 and figure 5 describe the domain of computational with boundary conditions and the mesh of computational, respectively.

The large cylindrical domain extended 4C and 8C upstream and downstream the rotor, respectively [20] to confirm that the boundaries doesn't influence on the flow at the turbine, Here, refinement grids with inflation are used near the blade surface to accurately capture the flow field inside the boundary layer. The grid is made up of unstructured tetrahedral mesh. The total number of cells in the computational domain is 2,614,335. The inlet and outlet conditions of computational domain are uniform velocity and outlet pressure, respectively. For the blades, hub and casing surfaces no slip wall conditions are used. Flow coefficient ϕ is changed from 0.1 to 0.325 and the fixed rotational speed of turbine (2000 rpm). Henceforth, the blade tip speed was kept constant.

Figure 6 shows the influence of number of cells in computational domain on the CFD results of turbine efficiency η at flow coefficient $\phi = 0.15$. The number of cells was gradually increased in five steps from 1,015,551 cells to 3,953,000 cells, with constant non-dimensional wall distance $y^+ < 1$ at the same ϕ . This study showed that the maximum percentage of the diffractions of torque coefficient C_T , total pressure loss coefficient C_p , and efficiency η are $\pm 0.99\%$, $\pm 0.66\%$ and $\pm 0.33\%$, respectively. Cells number of 2,614,335 is the best solution quality, where CFD results are independent of the number of cells in computational domain. Thus, this meshes number was utilized during the present study.

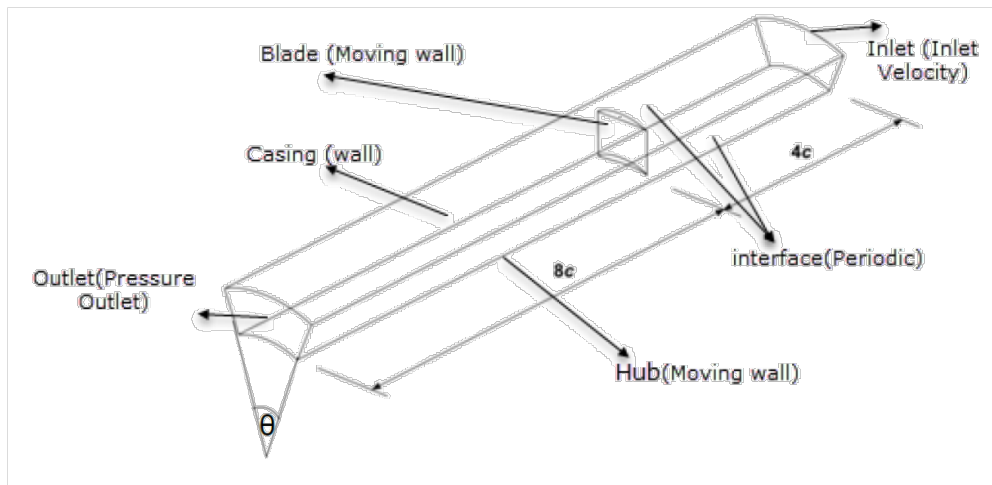


Figure 4. The computational domain with boundary conditions.

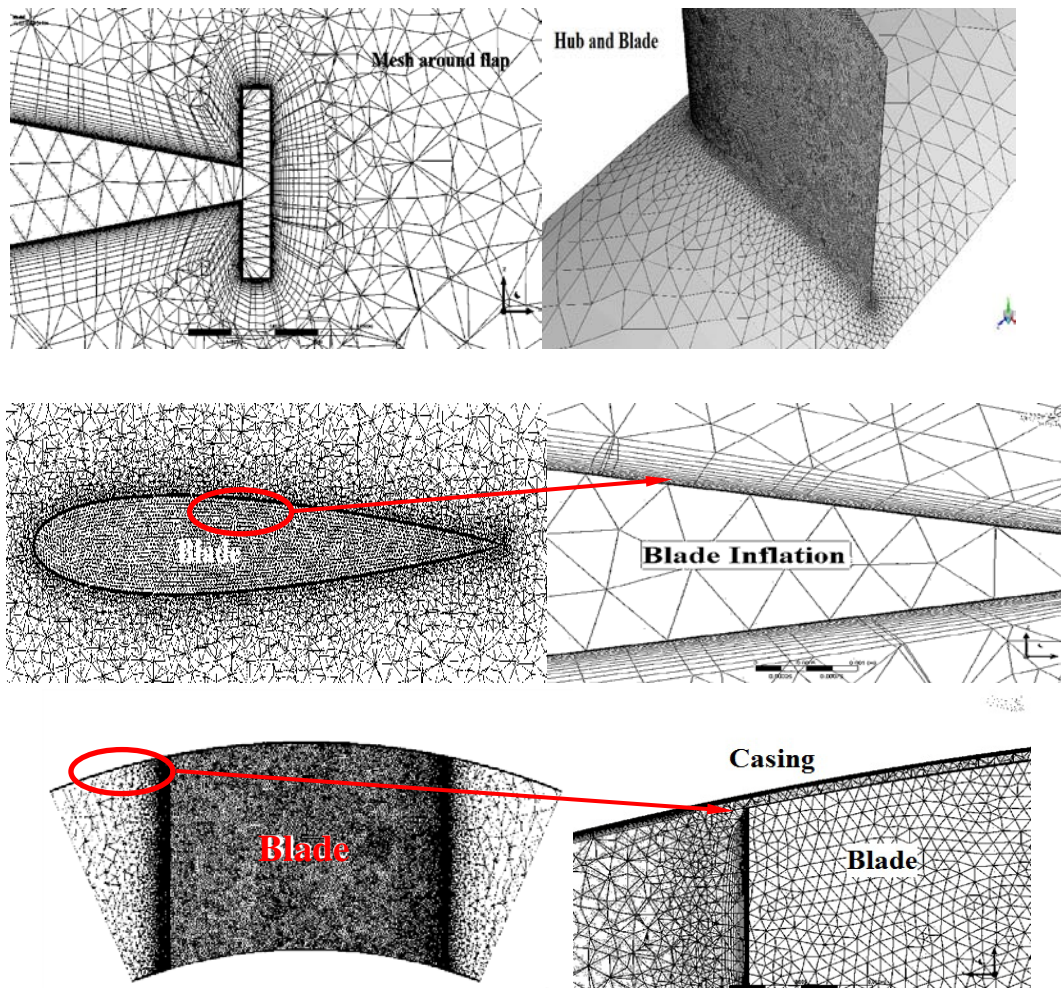


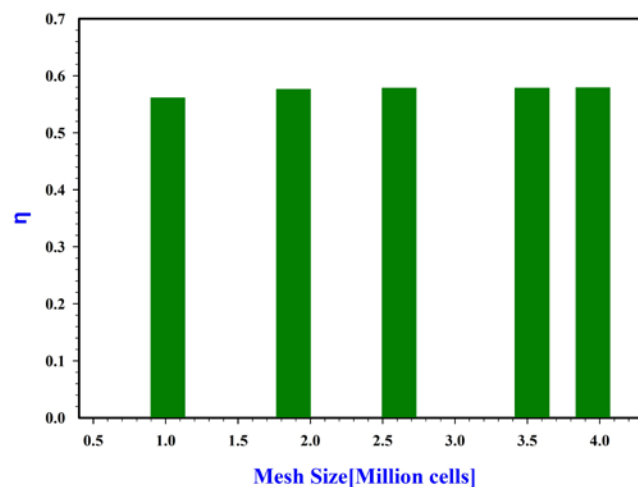
Figure 5. Unstructured/tetrahedral computational mesh.

Table 2. Specifications of turbine model.

Parameter	Dimension
Blade Profile	NACA0015
Number of blades, Z	8
Domain angle, θ	45°
Blade chord length, c	0.125 m
Blade thickness, t	0.01875 m (15% of c)
Hub diameter, D_t	0.4 m
Casing diameter, D_c	0.59 m
Tip clearance	0.001 m
Blade height, H	0.094 m
Solidity, σ	0.644
Stagger angle	90°
Turbine rotational speed, N	2000 rpm

Table 3. Meshing and boundary conditions.

Parameter	Description
Flow domain	Single blade
Interface	Periodic
Mesh/Nature	Unstructured/tetrahedral
Elements	2,614,335
Fluid	Air
Turbulence model	SST $k - w$
Inlet	Velocity
Outlet	Pressure
Hub	Wall
Casing	Wall
Blade	Wall
Maximum Residual criteria	1×10^{-4}

**Figure 6.** Influence of cells number on turbine efficiency.

3.2. Model validation

A validation curve of torque coefficient C_T , total pressure loss coefficient C_p , and efficiency η has been determined at different values of flow coefficient ϕ as shown in figures 7a, 7b, and 7c, respectively. The validation results were compared with both the experimental results [2] and CFD results [12, 21, 23 and 31]. The results of the present work show good agreement with the results of Curran and Gato [2]. Accordingly, the present CFD model has been great admitted as a computational tool for the performance of Wells turbine.

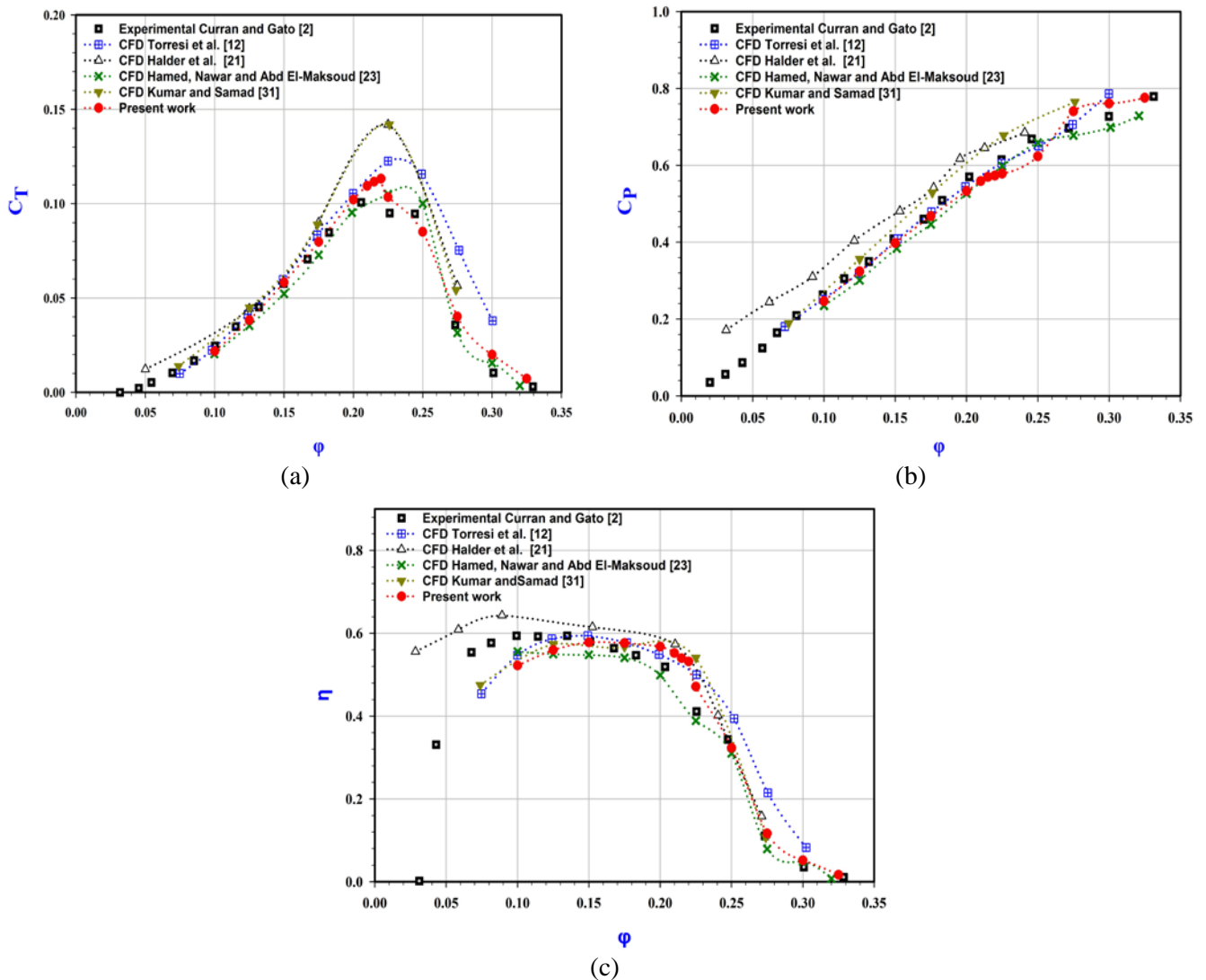


Figure 7. Validation with experimental and CFD results for: (a) C_T , (b) C_p , and (c) η .

Figure 8 presents the error percentage of the present work compared with the experimental results of Curran and Gato [2]. As it is depicted from the figure that the maximum error percentage for torque coefficient, the total pressure drop coefficient and efficiency are 9.9%, 7.3%, and 11.7%, respectively. It is notably to mention that the error percentage concerned the efficiency is dependent upon the errors of the torque and pressure drop coefficients.

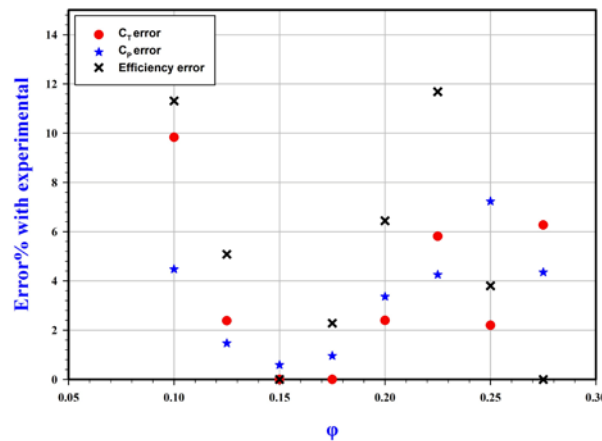


Figure 8. Error percentage with experimental results.

Validation of the rectangular flap at $FW = 0.5 \% C$ & $FH = 1.5 \% C$ is also achieved with Kumar and Samad [31] for more satisfaction. Figure 9 presents that the present CFD results have a good agreement with Kumar and Samad [31]. However, Kumar and Samad [31] studied only the effect of varying the rectangular flap height (FH) on the Wells turbine performance. So, in this paper, the effect of varying flap height (FH) and flap width (FW) on the Wells turbine performance has been considered.

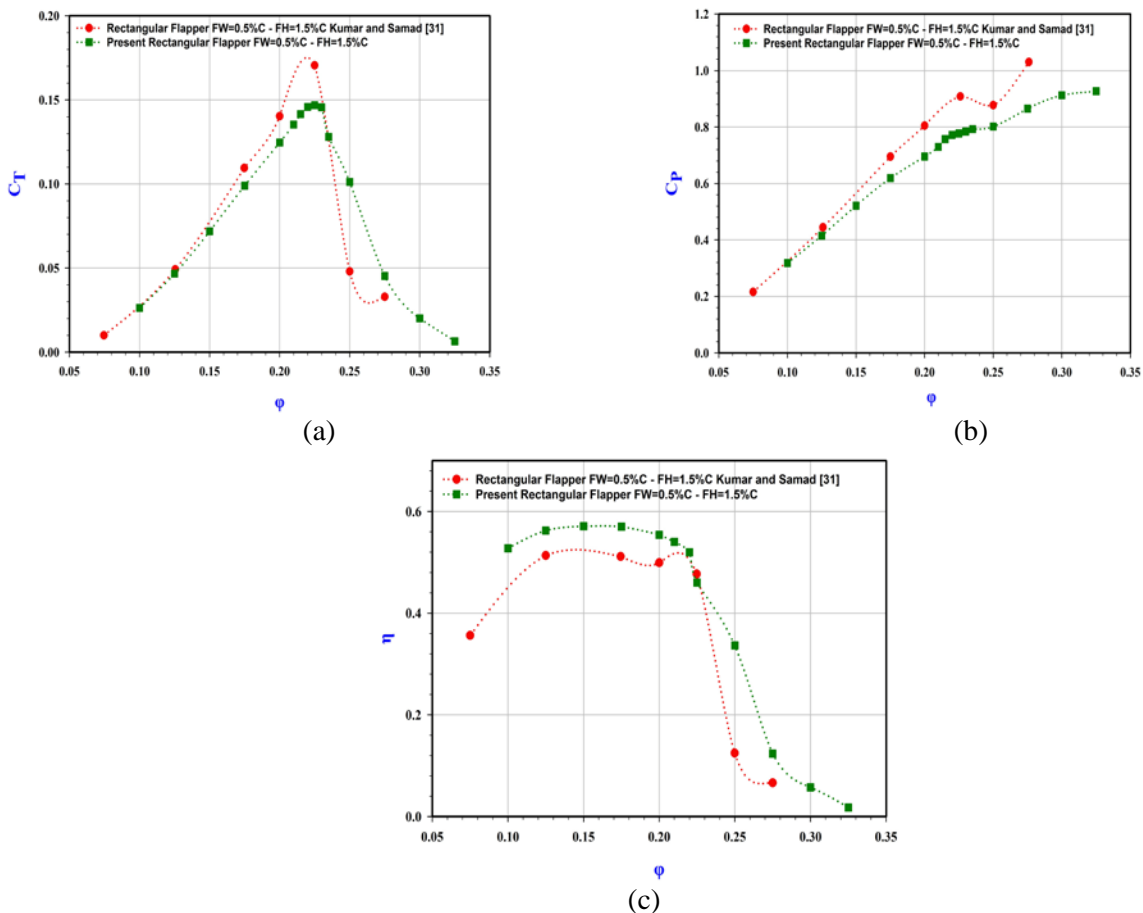


Figure 9. Verification of the present rectangular flapper results. For: (a) C_T , (b) C_p , and (c) η .

3.3. Effect of rectangular flap height

Figure 10 demonstrates the effect of rectangular flap height on the variations of C_T , C_p , and η at different values of ϕ . The results show that the rectangular flap of $FW = 0.5\%C$ & $FH = 1.5\%C$ gives a maximum value of $C_T = 0.148$ at $\phi = 0.225$. While, the maximum $C_T = 0.113$ at $\phi = 0.22$ for blade without flap ($FH = 0\%C$). Hence, the percentage increase in C_T is 41.98% at $\phi = 0.225$, see figure 10(a). On the other hand, C_p is increased as the flap height increases especially at the values of $\phi > 0.2$ as shown in figure 10(b). Despite the decrease in the efficiency compared with the blade without flap (reference case), the amount of power generated had been enhanced, figure 10(c).

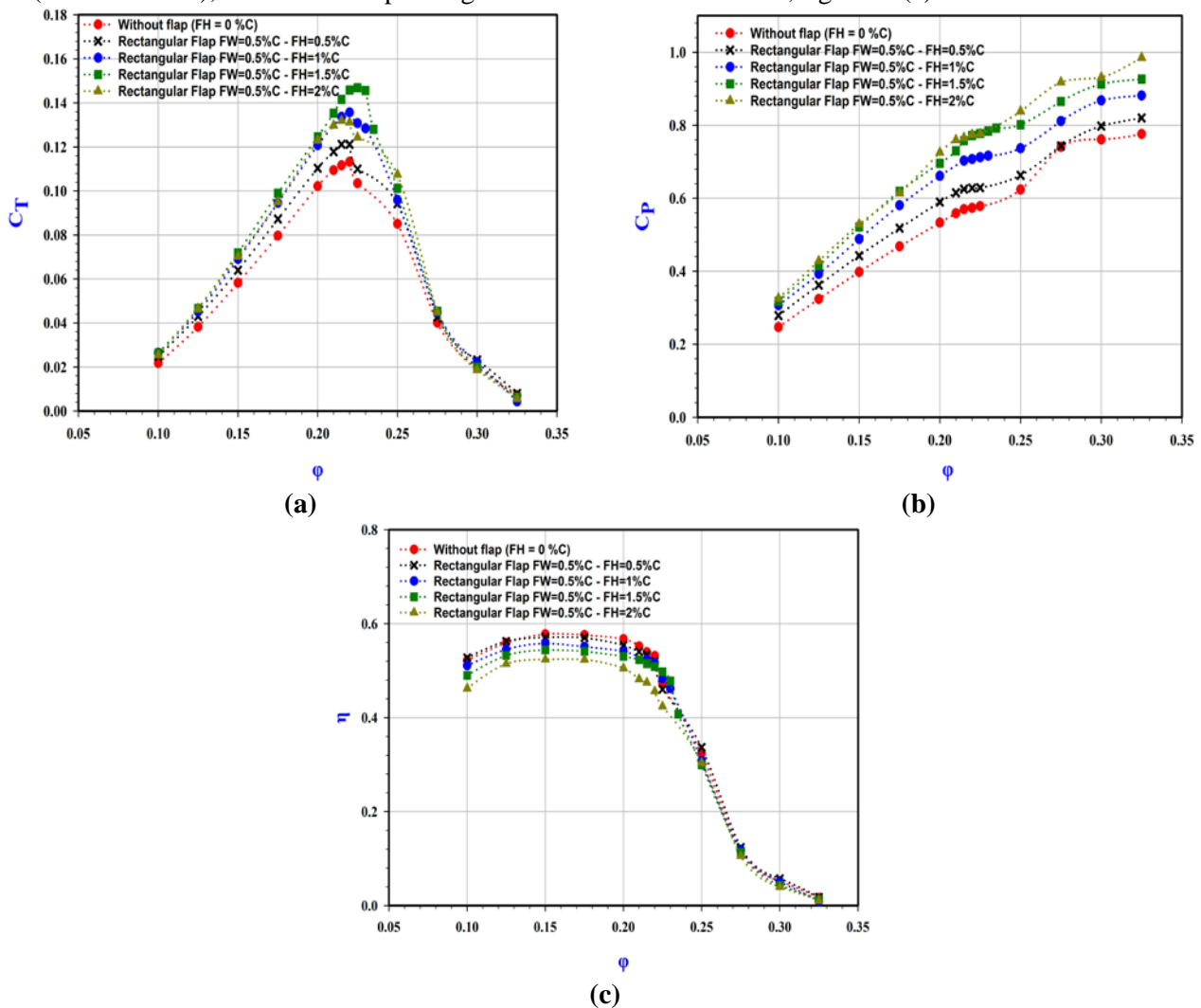


Figure 10. Effect of rectangular flap height (FH) on: (a) C_T , (b) C_p , and (c) η .

The velocity streamlines are presented for Wells turbine blade without flap ($FH = 0\%C$) and with flaps of different heights as shown in figure 11. The comparison of velocity streamlines between blades with flap is established at $FW = 0.5\%C$, $H = 50\%$, $\phi = 0.2$ and $FH = (0\%, 0.5\%, 1\%, 1.5\%, \text{ and } 2\%)$. It is noticed that, at the blade without flap ($FH = 0\%C$); a vortex is formed at the end of the trailing edge. This vortex separates the flow from the surface of the blade, which reduces the power generated, see figure 11 (a). The flap position at the end of the blades generates to vortices regions; a forward and backward. The forward vortices size is very small compared with the backward vortices, which diminish their effect. Hence, the backward vortices, that is located downstream the blade, made a low-pressure zone. This reduces the chance of the boundary layer separation and give the opportunity to entrain more streamlines that in turn enhance the power generated. Accordingly, the size and location of

the vortices have a very vital effect on the performance of the blades. The effect of flap of FH = 0.5 and 1 is very small compared with the flap of FH = 1.5 and 2 as shown in figures 11 (b, c, d, and e) respectively.

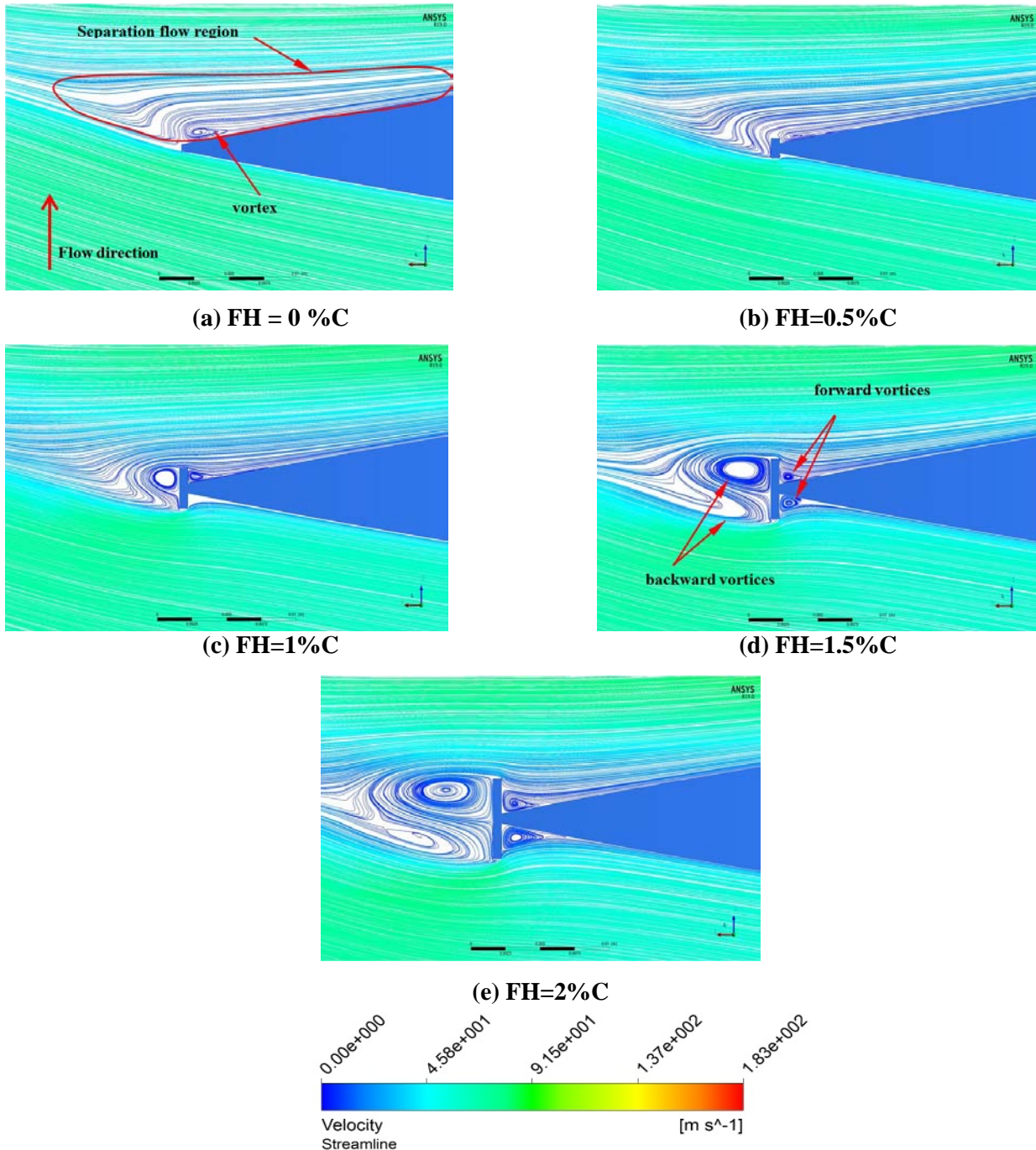


Figure 11. Velocity streamlines of rectangular flaps of different heights at FW=0.5%C, H=50% and $\Phi=0.2$.

3.4. Effect of rectangular flap width

Figure 12 illustrates the effect of rectangular flap width on the variations of C_T , C_P , and η at different values of ϕ . The rectangular flap of FW = 0.5 %C gives a maximum value of C_T at $\phi = 0.225$ compared with the other geometries as shown in figure 12(a). On the other hand, the rectangular flap of width

(FW = 0.4, 0.5, and 0.6 %C) approximately the same values of C_p through the range of ϕ as shown in figure 12(b). Despite the decrease in the efficiency compared with the blade without flap (FH = 0%), the amount of power generated had been enhanced, figure 12(c). therefore, the optimum rectangular flap dimensions are FH = 1.5 %C and FW = 0.5 %C

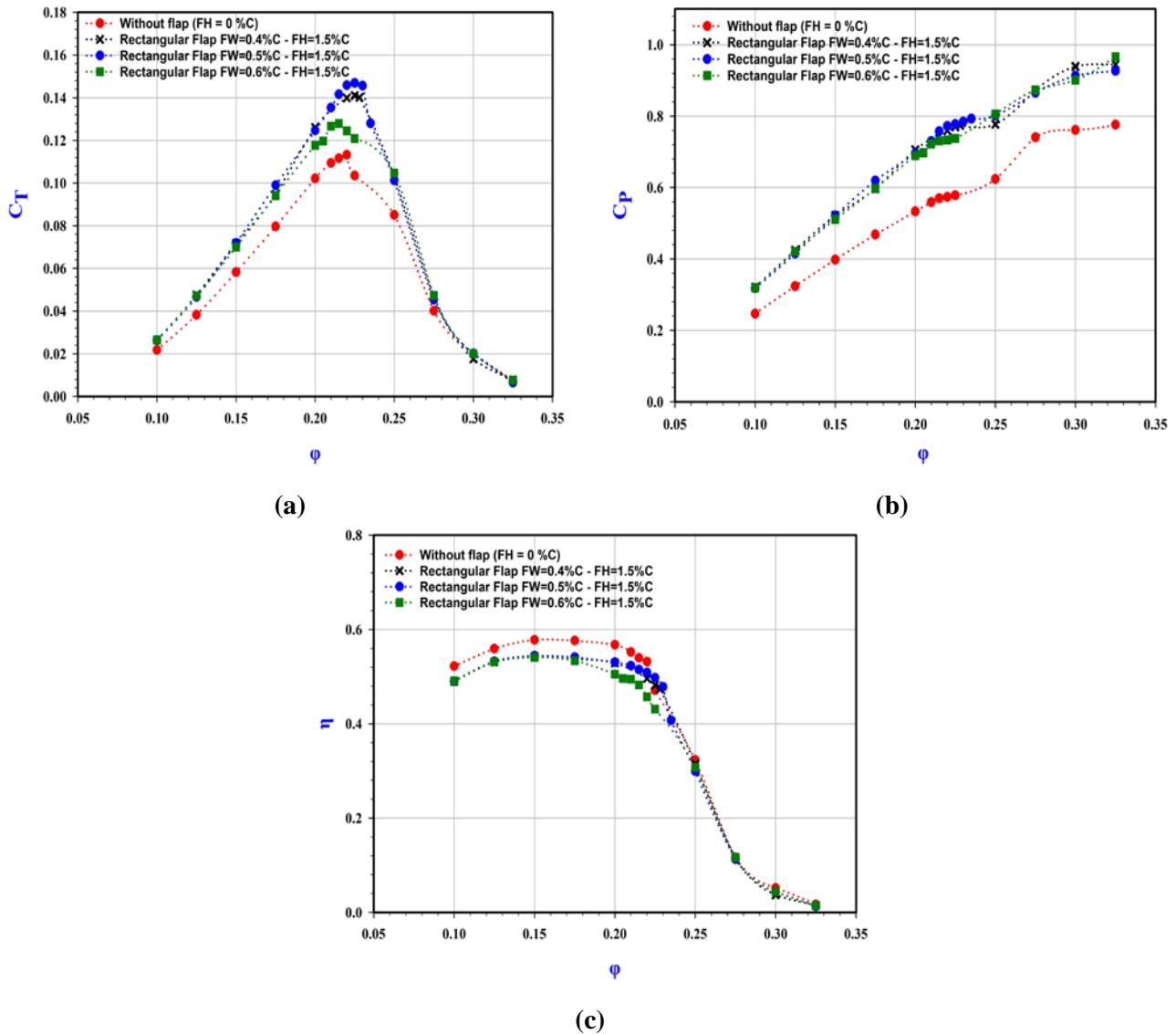


Figure12. Effect of rectangular flap width (FW) on: (a) C_T , (b) C_p , and (c) η .

The velocity streamlines are presented for Wells turbine blade without flap (FH = 0 %C) and with flaps of different widths as shown in Figure 13. The comparison of velocity streamlines between blades with flap is accomplished at FH = 1.5 %C, H = 50 %, $\phi = 0.2$ and FW = (0%, 0.4%, 0.5%, and 0.6%). The backward vortices that is formed at FW = 0.5% C is very dense compared to others, see figure 13 (C).

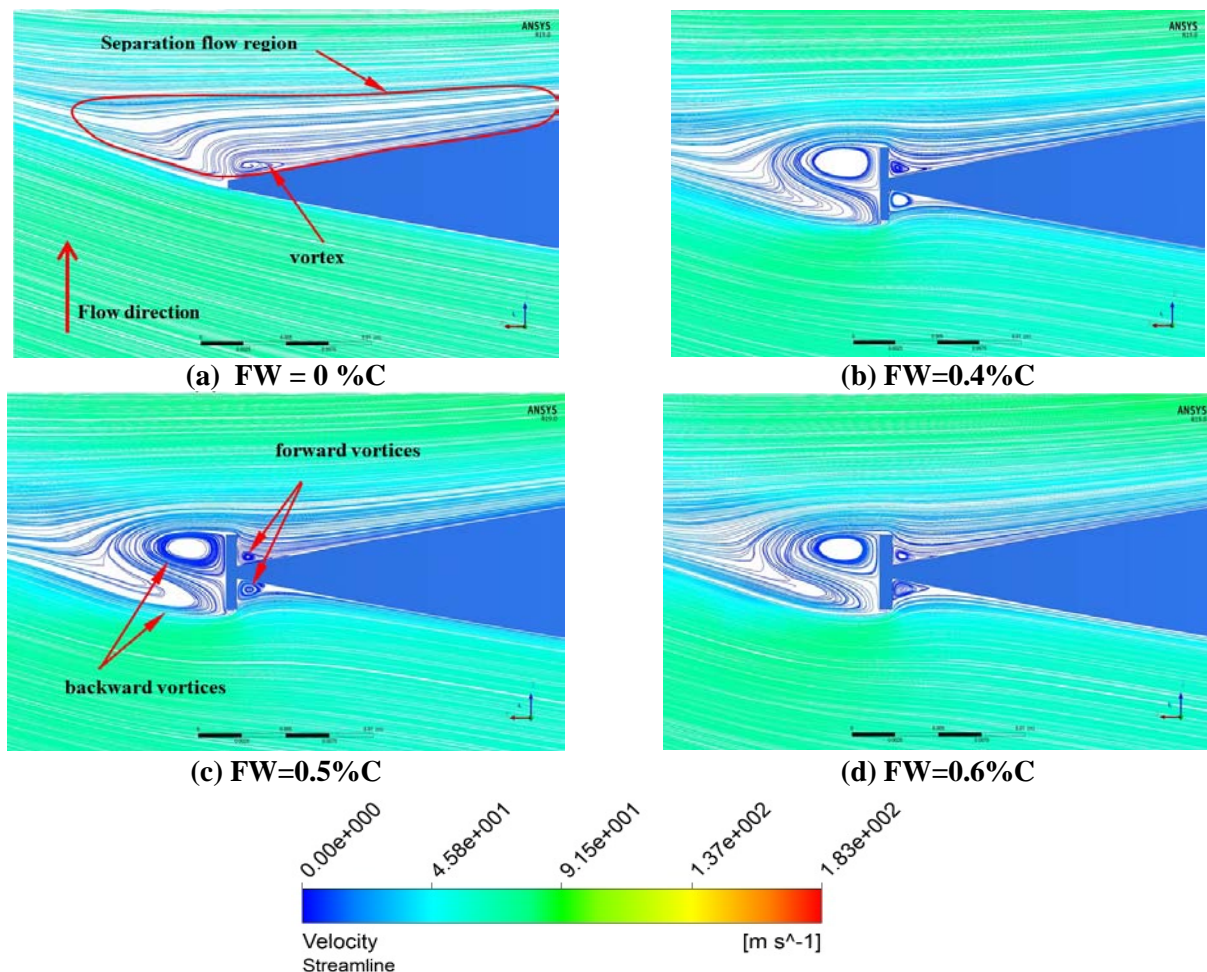


Figure 13. Velocity streamlines of rectangular flaps of different width at FH=1.5%C, H=50% and $\Phi=0.2$.

4. Conclusions

The aim of the present work is enhancing the Wells turbine performance. Rectangular Gurney flap has been elaborated herein. The turbine performance is investigated under steady unidirectional flow conditions using SST $k-\omega$ model where its numerical results were validated. The model is based on 3D incompressible RANS equation in the single rotating reference frame. Accordingly, the following conclusions are taken:

1. The Gurney flap generates two types of vortices; forward and backward vortices. The forward vortices size is very small compared with the backward vortices that diminish their effect.
2. The blade without flap achieves maximum torque coefficient equals to 0.113 at $\Phi = 0.22$. Furthermore, the stall inception appears at flow coefficient equals to 0.22.
3. Compared with the blade without flap, the blade with rectangular flap (FH = 1.5 %C and FW = 0.5 %C) achieves maximum torque coefficient equals to 0.148. Moreover, the stall point is delayed to flow coefficient equals to 0.225. Furthermore, the maximum percentage of increasing in the torque coefficient is 41.98% at such flow coefficient
4. The Gurney flap width (FW) does not affect on total pressure drop coefficient through the whole range of operation for rectangle flap.

References

- [1] Gato L, Warfield V and Thakker A 1996 Performance of a High-Solidity Wells Turbine for an OWC Wave Power Plant *Journal of Energy Resources Technology* **118** pp 263-268.
- [2] Curran R and Gato L 1997 The energy conversion performance of several types of Wells turbine designs *Proceedings of the Institution of Mechanical Engineers Part A: Journal of Power and Energy* **211** pp 133-145.
- [3] Kim T, Setoguchi T, Kaneko K and Raghunathan S 2002 Numerical investigation on the effect of blade sweep on the performance of Wells turbine *Renewable Energy* **25** pp 235-248
- [4] Setoguchi T, Takao M and Kaneko K 2000 A Comparison of Performances of Turbines for Wave Power Conversion *International Journal of Rotating Machinery* **6** pp129-134.
- [5] Setoguchi T and Takao M 2006 Current status of self rectifying air turbines for wave energy conversion *Energy Conversion and Management* **47** pp 2382-2396
- [6] Brito-Melo A, Gato L and Sarmiento A 2002 Analysis of Wells turbine design parameters by numerical simulation of the OWC performance *Ocean Engineering* **29** pp 1463-1477.
- [7] Dhanasekaran T and Govardhan M 2005 Computational analysis of performance and flow investigation on wells turbine for wave energy conversion *Renewable Energy* **30(14)** pp 2129-2147.
- [8] Raghunathan S, Setoguchi T and Kaneko K 1989 The Effect of Inlet Conditions on the Performance of Wells Turbine *Journal of Energy Resources Technology* **111(1)** pp 37-42.
- [9] Kim T, Setoguchi T, Kinoue Y and Kaneko K 2001 Effects of blade geometry on performance of wells turbine for wave power conversion *Journal of Thermal Science* **10(4)** pp 293-300.
- [10] Setoguchi T, Santhakumar S, Takao M, Kim T and Kaneko K 2003 A modified Wells turbine for wave energy conversion *Renewable Energy* **28(1)** pp 79-91.
- [11] Takao M, Setoguchi T, Kinoue Y and Kaneko K 2006 Effect of end plates on the performance of a wells turbine for wave energy conversion *Journal of Thermal Science* **15(4)** pp 319-323.
- [12] Torresi M, Camporeale S, Strippoli P and Pascazio G 2008 Accurate numerical simulation of a high solidity Wells turbine *Renewable Energy* **33(4)** pp 735-747.
- [13] Setoguchi T, Kim T, Takao M, Thakker A and Raghunathan S 2004 The effect of rotor geometry on the performance of a Wells turbine for wave energy conversion *International Journal of Ambient Energy* **25(3)** pp137-150.
- [14] Takao M, Thakker A, Abdulhadi R and Setoguchi T 2006 Effect of blade profile on the performance of a large-scale Wells turbine for wave-energy conversion *International Journal of Sustainable Energy* **25(1)** pp 53-61.
- [15] Thakker A, Dhanasekaran T and Ryan J 2005 Experimental studies on effect of guide vane shape on performance of impulse turbine for wave energy conversion *Renewable Energy* **30(15)** pp 2203-2219.
- [16] Setoguchi T and Takao M 2001 State of art on self-rectifying air turbines for wave energy conversion *Proceedings of the fourth international conference on mechanical engineering Dhaka Bangladesh* pp 117-126.
- [17] Boake C, Whittaker T, Folley M and Ellen H 2002 Overview and initial operational experience of the LIMPT wave energy plant *Proceedings of the 12th international offshore and polar engineering conference ISOPE Kitakyushu Japan vol 1* pp 586-594.
- [18] Taha Z and Sugiyono T 2010 A comparison of computational and experimental results of Wells turbine performance for wave energy conversion *Appl Ocean Res* **32** pp 83-90.
- [19] Taha Z, Sugiyono T, Ya T and Swada T 2011 Numerical investigation on the performance of Wells turbine with non-uniform tip clearance for wave energy conversion. *Appl Ocean Res* **33** pp 321-331.
- [20] Shaaban S and Abdel HA 2012 Effect of duct geometry on Wells turbine performance *J. Energy Convers Manag.* **61** pp 51-58.
- [21] Halder P and Samad A 2015 Casing Treatment of a Wave Energy Extracting Turbine *Aquatic Procedia* **4(Icwrcoe)** pp 516-521.

- [22] Thakker A and Abdulhadi R 2008 The performance of Wells turbine under bi-directional airflow *Renewable Energy* **33** pp 2467–2474.
- [23] Hamed H, Nawar M and Abd El-Maksoud R 2017 A New Operating Concept to Enhance Wells Turbine Performance *17th International Conference on Aerospace Sciences & Aviation Technology* 11-13 April Proceedings of the 17th Int. ASAT Conference Military Technical College Kobry Elkobbah Cairo Egypt.
- [24] Halder P, Samad A, Jinhyuk K, and Young C 2015 High performance ocean energy harvesting turbine design—A new casing treatment scheme *Energy* **86** pp 219-231.
- [25] Halder P and Samad A 2016 Optimal Wells turbine speeds at different wave conditions *International journal of marine energy* **16** pp133-149.
- [26] Halder P, Samad A and Thévenin D 2017 Improved design of a Wells turbine for higher operating range *Renewable energy* **106** pp122-134.
- [27] Halder P, Rhee SH and Samad A 2017 Numerical optimization of Wells turbine for wave energy extraction *International journal of naval architecture and ocean engineering* **9(1)** pp 11-24.
- [28] Torres FR, Teixeira PR and Didier E 2018 A methodology to determine the optimal size of a wells turbine in an oscillating water column device by using coupled hydro-aerodynamic models *Renewable Energy* **121** pp 9-18.
- [29] Nazeryan M and Lakzian E 2018 Detailed entropy generation analysis of a Wells turbine using the variation of the blade thickness *Energy* **143** pp385-405.
- [30] Gratton T, Ghisu T, Parks G, Cambuli F and Puddu P 2018 Optimization of blade profiles for the Wells turbine *Ocean Engineering* **169** pp 202-214.
- [31] Kumar P and Samad A 2019 Introducing Gurney Flap to Wells Turbine Blade and Performance Analysis with OpenFOAM *Ocean Engineering* **187** 106212

NOMENCLATURE

Abbreviations

LE	Leading edge	TE	Trailing edge
GF	Gurney flap	FH	Flap height
FW	Flap width	PS	Pressure side
SS	Suction side	RANS	Reynolds-averaged Navier-Stokes
OWC	Oscillating water column	SST	Shear stress transport
MRF	Moving Reference Frame	SIMPLEC	Semi-Implicit Method for Pressure-Linked Equations-Consistent

Symbols

C	Chord length (m)	K	Turbulence kinetic energy (m^2/s^2)
H	Blade height (m)	y^+	Non-dimensional wall distance(–)
R_T	Rotor tip radius (m)	F_t	Tangential force (N)
R_h	Rotor hub radius (m)	F_a	Axial force (N)
R_c	Casing radius (m)	T	Torque (Nm)
R_m	Rotor mean radius (m)	Q	Volume flow rate (m^3/s)
T	Blade thickness (m)	U	Rotor tip speed (m/s)
Z	Number of blades	C_x	Axial velocity (m/s)
σ	Turbine solidity	W	Relative velocity (m/s)
C_T	Torque coefficient (–)	Δp_o	Total pressure drop (Pa)
C_P	Total pressure drop coefficient (–)	ω	Angular velocity (rad/s)
\emptyset	Flow coefficient (–)	ρ	Air density (kg/m^3)
η	Efficiency (–)	α	Incidence angle ($^\circ$)
L	Lift force (N)	*	Non-dimensional parameter